Regulation of *pyr* Gene Expression in *Mycobacterium smegmatis* by PyrR-Dependent Translational Repression[▽]

Christopher J. Fields and Robert L. Switzer*

Department of Biochemistry, University of Illinois, Urbana, Illinois 61801

Regulation of pyrimidine biosynthetic (*pyr*) genes by a transcription attenuation mechanism that is mediated by the PyrR mRNA-binding regulatory protein has been demonstrated for numerous gram-positive bacteria. Mycobacterial genomes specify *pyrR* genes and contain obvious PyrR-binding sequences in the initially transcribed regions of their *pyr* operons, but transcription antiterminator and attenuation terminator sequences are absent from their *pyr* 5′ leader regions. This work demonstrates that repression of *pyr* operon expression in *Mycobacterium smegmatis* by exogenous uracil requires the *pyrR* gene and the *pyr* leader RNA sequence for binding of PyrR. Plasmids containing the *M. smegmatis pyr* promoter-leader region translationally fused to *lacZ* also displayed *pyrR*-dependent repression, but transcriptional fusions of the same sequences to a *lacZ* gene that retained the *lacZ* ribosome-binding site were not regulated by PyrR plus uracil. We propose that PyrR regulates *pyr* expression in *M. smegmatis*, other mycobacteria, and probably in numerous other bacteria by a translational repression mechanism in which nucleotide-regulated binding of PyrR occludes the first ribosome-binding site of the *pyr* operon.

The genes of de novo pyrimidine nucleotide biosynthesis (*pyr* genes) are regulated in many diverse bacteria by the *pyr* mRNA-binding regulatory protein PyrR (33). The mechanism by which PyrR regulates the expression of *pyr* genes has been studied in *Bacillus* (17–19, 35, 36), *Enterococcus* (13), *Lactococcus* (20, 21), and *Lactobacillus* (4, 12, 25) species. In these organisms PyrR acts by mediating a nucleotide-regulated transcription attenuation mechanism, which has been well characterized in genetic and biochemical studies with *Bacillus subtilis* (33) and *Bacillus caldolyticus* (8, 14). PyrR binds to *pyr* mRNA at a site which lies upstream of the genes that it regulates. This site, called the binding loop, consists of an RNA stem-loop with a purine-rich internal loop in the 5′ strand that contains two segments of highly conserved nucleotide sequence (6). Thus, PyrR-binding loops are readily identified by examination of the DNA sequences at the 5′ untranslated regions of *pyr* genes. Furthermore, the attenuation mechanism requires the presence of two additional RNA secondary structures that lie immediately downstream from the binding loop. These are the attenuator, which is a typical bacterial factor-independent terminator, and an upstream antiterminator, a stem-loop structure whose formation prevents formation of the attenuator stem-loop. Binding of PyrR to the binding loop occludes the 5′ strand of the antiterminator, permitting the formation of the attenuator, which results in premature termination of transcription and reduced expression of the downstream *pyr* genes. Thus, binding of PyrR, which is stimulated by uridine nucleotides, leads to repression, whereas the antagonism of binding by guanosine nucleotides leads to cross-regulatory derepression of *pyr* gene expression (8).

Sequencing of the genomes of a number of *Mycobacterium* species has revealed that most of their *pyr* genes are organized into an operon in which the first gene encodes a PyrR homolog and an obvious binding loop sequence lies immediately upstream of the *pyrR* open reading frame (7, 9, 32) (GenBank accession no. CP000480 for the *M. smegmatis* genome) (Fig. 1A). However, sequences encoding attenuator (terminator) and antiterminator structures are not found in the *pyr* leader region (Fig. 1B), which makes it highly unlikely that mycobacterial *pyr* genes are regulated by the transcription attenuation mechanism described above. If PyrR participates in the regulation of *pyr* genes in mycobacteria, an indication as to how it might do so comes from the observation that the binding loop sequence overlaps the Shine-Dalgarno sequence of a putative ribosome-binding site for the *pyrR* gene (Fig. 1A). Binding of PyrR to the binding loop might prevent binding of ribosomes and thus inhibit translation of the gene. If the binding of PyrR to the binding loop is in turn regulated by nucleotides as in other bacteria, a means would be provided for regulation of translation of *pyrR* and, via translational coupling, of downstream *pyr* genes.

In this work evidence is presented that (i) the expression of *pyr* genes is repressed by exogenous uracil in *Mycobacterium smegmatis*, (ii) repression of *pyr* genes requires the presence of both the *pyrR* gene and the binding loop RNA sequence to which PyrR binds, and (iii) PyrR-dependent regulation is mediated by a translational repression mechanism. We propose that these generalizations apply to other mycobacterium species as well.

MATERIALS AND METHODS

Bacterial strains and culture conditions. *M. smegmatis* and *Escherichia coli* strains used are listed in Table 1. *M. smegmatis* cultures were maintained on Middlebrook 7H9 broth medium and 7H10 solid medium (Difco) and were supplemented with ADC supplement (1× final concentration; Difco); liquid medium was supplemented with 0.05% Tween 20 to inhibit cell clumping. Where noted, the following supplements and antibiotics were added (final concentra-

* Corresponding author. Mailing address: Department of Biochemistry, University of Illinois, 600 South Mathews, Urbana, IL 61801. Phone: (217) 333-3940. Fax: (217) 244-5858. E-mail: rswitzer@uiuc.edu.
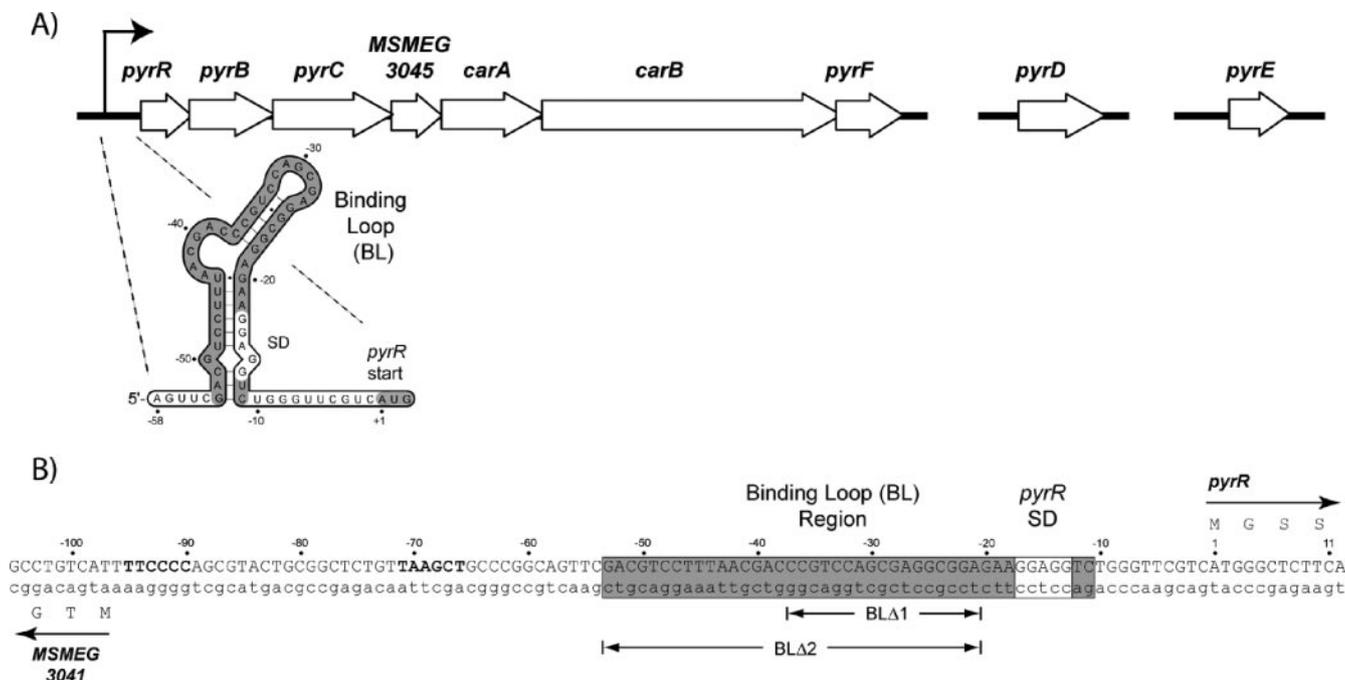
FIG. 1. A. Schematic diagram of the chromosomal organization of the pyrimidine biosynthetic (*pyr*) genes in *M. smegmatis*. The *pyrRBC-orf3045-carAB-pyrF* operon is shown at the left; the *pyrD* and *pyrE* genes are unlinked and located away from the *pyr* operon. MSMEG3045 denotes an open reading frame of unknown function. The bent arrow indicates the start of transcription of the operon. A portion of the promoter-leader region of the transcript shown below illustrates the predicted secondary fold of the PyrR-binding loop (BL; shaded) in the RNA, the Shine-Dalgarno sequence of a putative ribosome binding site (SD), and start codon (shaded AUG) for *pyrR*, the first gene of the operon. B. DNA sequence on the *pyr* operon promoter-leader region; the nontemplate strand is shown in capital letters. The sequence is numbered with the first base of the *pyrR* start codon as +1. The sequence specifying the PyrR-binding loop is enclosed in a box and shaded, except for a box designating the putative Shine-Dalgarno sequence. Putative −35 and −10 promoter sequences are shown in boldface. MSMEG3041 indicates an open reading frame of unknown function (annotated as a member of the thiopurine *S*-methyltransferase family) that is transcribed in an opposite direction to the *pyr* operon. Regions deleted from the binding loop in *pyr′-lacZ* fusion plasmids pFS20 and pFS22 are denoted by Δ1; those deleted in *pyr′-lacZ* fusion plasmids pFS21 and pFS23 are denoted by Δ2.

tions in parentheses): kanamycin (50 μg/ml for both *E. coli* and *M. smegmatis*), gentamicin (10 μg/ml for both *E. coli* and *M. smegmatis*), ampicillin (100 μg/ml for *E. coli* only), uracil (100 μg/ml), uridine (200 μg/ml), L-arginine (50 μg/ml), sucrose (10%), 5-bromo-4-chloro-3-indoyl-β-D-galactoside (X-Gal; 50 μg/ml). When β-galactosidase and aspartate transcarbamylase activities were measured, the cultures were grown in 25 ml of Middlebrook medium in 125-ml sidearm flasks with aeration (250 rpm in a New Brunswick shaker). Growth was monitored using a Klett-Summerson meter with a no. 54 filter. Cells were harvested by centrifugation at early to mid-log phase at 60 to 75 Klett units; cell pellets were quickly frozen in liquid N$_2$ and stored at −20°C prior to analysis.

General techniques. All PCRs were performed using Platinum *Pfx* DNA polymerase (Invitrogen) and chemically synthesized primers. Plasmid clones were verified by sequencing (University of Illinois Core Sequencing Facility). The identities of plasmids transformed into *M. smegmatis* strains were verified by breaking a sample of the isolated clones using a Mini-BeadBeater (BioSpec, Inc.) and transforming *E. coli* DH5α with 5 to 10 μl of the supernatant; DNA isolated from *E. coli* transformants was then sequenced for verification.

Rapid screening of mycobacterial colonies for chromosomal rearrangements was performed using a modified colony PCR method (28). A small sample of a representative isolated colony was picked using a sterile pipette tip and added to 50 μl of distilled H$_2$O, vortexing briefly. The resuspended cells were incubated at 95°C for 5 min, followed by a second round of vortexing and incubation at 95°C. Cell debris was centrifuged for 10 min at 14,000 × *g*, and 2 to 5 μl of the resulting supernatant was used directly in the amplification reaction mixture.

Preliminary *M. smegmatis* genome sequence data were obtained from The Institute for Genomic Research website at http://www.tigr.org. The GenBank accession number for the genome sequence is CP000480.

Construction of *lacZ* transcriptional and translational fusion plasmids. All *lacZ* fusion plasmids were constructed as follows and as detailed in Table 1. Primers flanking the region of interest were used to amplify DNA from the

indicated template DNA (Table 1). Amplified DNA was gel purified, cut using ApaI and KpnI, and cloned into pJEM13 (translational fusion), pJEM15 (transcriptional fusions), or both to generate the indicated plasmid fusions. Plasmids were transformed into *M. smegmatis* by electroporation (15).

Construction of plasmids with PyrR-binding loop deletions BLΔ1 and BLΔ2. A fragment of 513 bp specifying the entire *M. smegmatis pyr* promoter region and DNA upstream of it was amplified by PCR and cloned into pZErO2.1, generating pFS11. Two deletion variants were constructed by inverse PCR. Amplified DNA was gel purified, phosphorylated using T4 polynucleotide kinase (Promega), and self-ligated to generate pFS16 (BLΔ1) and pFS18 (BLΔ2) (Table 1). The structures of the resulting deletion regions were verified by sequencing, and they were subcloned as described above into pJEM13 and pJEM15 (generating pFS20 to pFS23) (Table 1).

Construction of *M. smegmatis* Δ*pyrD* mutant strain CF1. The *M. smegmatis pyrD* gene was cloned by PCR amplification of 2,972 bp from the chromosomal *pyrD* region. The PCR fragment was digested with XbaI and HindIII and cloned into similarly cut pZErO2.1 to generate plasmid pFS3 (Table 1). A *pyrD* in-frame deletion plasmid was generated by digesting pFS3 with AgeI and BlpI (New England BioLabs) followed by a fill-in reaction using Klenow fragment of *E. coli* DNA polymerase (Promega), which regenerated the AgeI restriction site. This fragment was self-ligated to generate pFS3Δ1 (Table 1). Subsequent attempts at creating a markerless chromosomal *pyrD* deletion using *sacB*-based counterselection methods (16) were unsuccessful (data not shown). In order to create a marked allele for easier isolation of a *pyrD* mutant, a SmaI fragment from pGMΩ1 containing a gentamicin resistance gene in an omega interposon was ligated to AgeI-digested, blunt-ended pFS3Δ1 to generate pFS3Δ2. This plasmid is both kanamycin and gentamicin resistant and unable to replicate in *M. smegmatis*.

Allelic exchange experiments using pFS3Δ2 were conducted by electrotransformation of *M. smegmatis* mc^{2}155 using 2 μg of plasmid DNA treated with 100 kJ/cm^2 of UV irradiation to increase the frequency of recombination, as de-

TABLE 1. Bacterial strains and plasmids

Strain or plasmid	Description[a]	Reference or source
M. smegmatis strains		
mc²155	Parent strain; ATCC 700084	31
CF1	Derivative of mc²155; Δ*pyrD*::*gm* Gm^r	This work
CF22	Derivative of mc²155; Δ*pyrR*	This work
CF24	Derivative of CF1; Δ*pyrR* Δ*pyrD*::*gm* Gm^r	This work
E. coli strain		
DH5α	*recA1 endA1 gyrA96 thi-1 relA1 hsdR17*(r_K⁻ m_K⁺) *supE44* φ80*lacZ*Δ*M15* Δ(*lacZYA-argF*)*U169*	28
Plasmids		
pJEM13	*E. coli-Mycobacterium* translational *lacZ* reporter shuttle vector; Km^r	34
pJEM15	*E. coli-Mycobacterium* transcriptional *lacZ* reporter shuttle vector; Km^r	34
pZErO2.1	Cloning vector; Km^r	Invitrogen
p2NIL	Cloning vector; Km^r	26
pGOAL19	Plasmid carrying *lacZ*, *sacB*, and *hyg* genes in a PacI cassette; Ap^r Hyg^r	26
pGMΩ1	Plasmid carrying the *aacC1* omega interposon in a SmaI cassette; Gm^r	30
pFS1	*M. smegmatis pyrR* in pZERO2.1; Km^r	This work
pFS3	*M. smegmatis pyrD* in pZERO2.1; Km^r	This work
pFS3Δ1	*pyrD* in-frame deletion in pZERO2.1; Km^r	This work
pFS3Δ2	pFS3Δ1 *pyrD* in-frame deletion with omega interposon; Km^r Gm^r	This work
pFS4	pJEM13 with −488 to +9[b] of *pyrR* gene; Km^r	This work[c]
pFS5	pJEM13 with −233 to +9 of *pyrR* gene; Km^r	This work[c]
pFS6	pJEM13 with −102 to +9 of *pyrR* gene; Km^r	This work[c]
pFS8	pJEM15 with −488 to +9 of *pyrR* gene; Km^r	This work[c]
pFS9	pJEM15 with −233 to +9 of *pyrR* gene; Km^r	This work[c]
pFS10	pJEM15 with −102 to +9 of *pyrR* gene; Km^r	This work[c]
pFS11	pZErO2.1 with −488 to +9 of *pyrR* gene; Km^r	This work
pFS14	pFS1 derivative, *pyrR* in-frame deletion; Km^r	This work
pFS16	pFS11 derivative, binding loop deletion (BLΔ1); Km^r	This work
pFS18	pFS11 derivative, binding loop deletion (BLΔ2); Km^r	This work
pFS19	*pyrR* in-frame deletion cloned in p2NIL; Km^r	This work
pFS20	pJEM13 with −233 to +9 of *pyrR* gene, BLΔ1); Km^r	This work[d]
pFS21	pJEM13 with −233 to +9 of *pyrR* gene, BLΔ2); Km^r	This work[e]
pFS22	pJEM15 with −233 to +9 of *pyrR* gene, BLΔ1; Km^r	This work[d]
pFS23	pJEM15 with −233 to +9 of *pyrR* gene, BLΔ2; Km^r	This work[e]
pFS24	pFS19 with pGOAL19 PacI cassette; Km^r Hyg^r	This work
pFS28	pJEM15 with −488 to +579 of *pyrR* gene (includes intact *pyrR*); Km^r	This work[c]
pFS30	pJEM15 with *MSMEG_3041* promoter; Km^r	This work[c]
pFS31	pJEM15 with *Ag80* promoter; Km^r	This work[f]
pFS32	pJEM15 with *groEL2* (*hsp60*) promoter; Km^r	This work[f]

[a] Km^r, kanamycin resistance; Ap^r, ampicillin resistance; Gm^r, gentamicin resistance; Hyg^r, hygromycin resistance.
[b] Coordinates are relative to the *pyrR* translational start codon.
[c] PCR template was pFS1.
[d] PCR template was pFS16.
[e] PCR template was pFS18.
[f] PCR template was pGOAL19.

scribed previously (15). Single-crossover integrants from each transformation were selected on 7H10 plates supplemented with uracil, gentamicin, and kanamycin. Several independent single-crossover integrants were grown overnight under nonselective conditions in 7H9 broth with uracil and plated on 7H10 plates supplemented with uracil and gentamicin. Several hundred colonies were screened for potential double crossovers by kanamycin sensitivity via replica plating. From those, 20 colonies demonstrated the expected antibiotic sensitivity; these were subsequently replica plated to 7H10 plates with and without uracil. From that pool, one colony demonstrated a requirement for uracil for growth. This strain was designated CF1 (Table 1) and was used for all subsequent experiments.

Construction of *M. smegmatis* Δ*pyrR* strain CF22 and Δ*pyrR* Δ*pyrD* strain CF24. Plasmid pFS1 (Table 1), containing the wild-type *M. smegmatis pyrR* gene, was constructed by PCR amplification of 1,984 bp of the chromosomal *pyr* gene region. The PCR amplicon was gel purified, cut with HindIII and XbaI, and ligated into similarly cut pZErO2.1 (Table 1) to generate pFS1. An in-frame deletion of the *M. smegmatis pyrR* gene was constructed by digesting plasmid pFS1 with BbsI and PshAI followed by a fill-in reaction using Klenow fragment and subsequent religation, resulting in plasmid pFS14. After verifying the in-frame deletions by sequencing, the fragment was cloned into HindIII- and ScaI-

digested p2NIL (26) to generate plasmid pFS19. A PacI cassette containing *sacB*, *lacZ*, and hygromycin resistance genes was cloned from pGOAL19 (26) into pFS19 to generate the final knockout vector, pFS24 (Table 1).

pFS24 DNA (5 μg) was UV treated and electrotransformed into *M. smegmatis* strains mc²155 and CF1. Single-crossover plasmid integrants were selected on 7H10 medium containing uracil, arginine, X-Gal, and kanamycin. Several candidate single-crossover integrants (blue colonies) were screened by colony PCR to verify the presence of both *pyrR* alleles. Once verified, integrants were grown overnight in 7H9 broth with uracil and arginine, and dilutions were plated onto 7H10 plates containing 10% sucrose and uracil. After 3 to 5 days of growth, colonies were replica plated onto 7H10 plates containing sucrose, uracil, and X-Gal. Double-crossover candidates (white colonies) were further analyzed by colony PCR for the presence of the deletion allele only, using both bacterial strains (mc²155 and CF1) and plasmids (pFS1 and pFS24) as controls. Aspartate transcarbamylase (ATCase) assays were performed as a secondary screen to detect altered *pyr* gene expression. Strains CF22 (parent strain mc²155) and CF24 (parent strain CF1) were shown by colony PCR to contain the expected deletion in *pyrR* and by assay to display elevated ATCase activity when grown with uracil (Table 1).

TABLE 2. Repression of *M. smegmatis pyrB* (ATCase) by uracil and derepression by pyrimidine-limiting growth on uridine require the *pyrR* gene

Function	Strain	Strain genotype	Plasmid genotype	Chromosomally encoded ATCase			Plasmid-encoded β-galactosidase		
				Sp act (nmol/min/mg)		Ratio	Sp act (nmol/min/mg)		Ratio
				Uracil	NE or uridine[a]		Uracil	NE[a] or uridine	
Repression	mc²155	Wild type	NA[b]	7.7 ± 0.2	19 ± 1.6	2.5	–	–	–
	CF22	Δ*pyrR*	NA	64 ± 2.7	66 ± 4.1	1.0	–	–	–
	CF22/pJEM15[c]	Δ*pyrR*	None	64.5 ± 4.6	64.5 ± 2.9	1.0	3.5 ± 0.4	4.2 ± 1.9	1.2
	CF22/pFS28[d]	Δ*pyrR*	*pyrR-pyrB'-lacZ*	11 ± 0.8	20 ± 2.0	1.8	500 ± 27	540 ± 6.9	1.1
Derepression	CF1	Δ*pyrD*	NA	9 ± 1.4	130 ± 6.2	14	–	–	–
	CF24	Δ*pyrD* Δ*pyrR*	NA	69 ± 1.9	150 ± 7.8	2.2	–	–	–
	CF24/pJEM15	Δ*pyrD* Δ*pyrR*	None	60 ± 1.4	180 ± 15	3.0	1.3 ± 0.1	6.8 ± 0.5	5.2
	CF24/pFS28	Δ*pyrD* Δ*pyrR*	*pyrR-pyrB'-lacZ*	9.1 ± 0.6	130 ± 21	14	470 ± 19	6,000 ± 260	13

[a] NE, no effector (for strains mc²155 and CF22); uridine was used for derepression of strains CF1 and CF24.
[b] NA, not applicable.
[c] pJEM15 is the vector plasmid (promoterless *lacZ*).
[d] pFS28 is derived from pJEM15 and contains the *pyr* promoter region, *pyrR*, and the 5′ end of *pyrB* fused transcriptionally to *lacZ* (see text for details).

Assays. ATCase activity was monitored using a variation of the ¹⁴C-based radioassay (27) under assay conditions similar to those described for previous studies on the *M. smegmatis* ATCase (22). Frozen cell pellets were thawed on ice and washed three times with 50 mM Tris-acetate (pH 7.5), resuspended in the same buffer with 0.1-mm glass zirconium beads, and then disrupted by a single 90-s pulse using a Mini-BeadBeater. Beads and cell debris were removed by a 10-min centrifugation (14,000 × *g*), and the supernatant was used in assays. ATCase assays were performed at 30°C in a 100-μl final volume containing the following: 50 mM Tris-acetate (pH 7.5), 10 mM [¹⁴C]aspartate (final specific activity, 50 μCi/mmol; Amersham Biosciences), and 5 mM carbamoyl-phosphate (Sigma). Reactions were initiated by addition of enzyme and stopped with 900 μl 0.2 N acetic acid after 30 min. A 950-μl portion of each reaction mixture was added to a column containing Dowex AG-50W-X8 (200 to 400 mesh hydrogen form; Bio-Rad) to retain unreacted aspartate. Columns were washed four times with 400 μl 0.2 N acetic acid with the eluate collected in scintillation vials. Aquasol-2 (Packard Research) was added to the collected eluate, and total counts were determined using liquid scintillation counting.

For β-galactosidase assays the cells were grown and treated as for ATCase assays. In experiments where only β-galactosidase activity was determined, the cells were resuspended in Z buffer lacking 2-mercaptoethanol (24) prior to breaking in the Mini-BeadBeater as described above; in experiments where both ATCase and β-galactosidase were determined, 50 mM Tris-acetate was used as the breaking buffer to avoid possible phosphate inhibition of ATCase activity. β-Galactosidase activity was determined as described previously (34) using Z buffer containing 40 mM β-mercaptoethanol.

Protein concentrations were determined using the BCA protein assay kit (Pierce), using bovine serum albumin as the protein standard.

RESULTS

Repression of *M. smegmatis pyr* genes by exogenous uracil requires the *pyrR* gene. ATCase is encoded by *pyrB*, the second gene in the *M. smegmatis pyr* operon (Fig. 1A). Assays of ATCase activity were used to measure the level of *pyr* operon expression in *M. smegmatis* cells grown under repressing and derepressing conditions. The repressive effects of exogenous uracil on ATCase levels in the parent strain, mc²155, were modest, only about twofold (Table 2). When a pyrimidine auxotroph derived from mc²155, strain CF1 (Δ*pyrD*), was grown with uridine as the pyrimidine source, growth was very slow (doubling time of 18 h compared to 4.7 h when this strain was grown with uracil supplementation), which indicates very poor utilization of exogenous uridine by *M. smegmatis* with consequent starvation for pyrimidines. With strain CF1, pyrimidine-limited growth led to a 14-fold derepression of AT-

Case, relative to the repressed level in cells grown with uracil (Table 2). Thus, expression of the *pyr* operon is clearly regulated by the supply of exogenous pyrimidines, presumably acting via effects on the intracellular concentration of pyrimidine nucleotides.

Repression of *pyr* expression was dependent on the presence of an intact *pyrR* gene. This was demonstrated by determination of the levels of ATCase activity in strain CF22, a derivative of strain mc²155 containing an in-frame deletion of the *pyrR* gene. ATCase specific activity was eightfold higher in CF22 cells than in the repressed *pyrR*⁺ parent strain and was not repressed by growth of the cells in the presence of uracil (Table 2). The ATCase level in strain CF24, a Δ*pyrR* derivative of the Δ*pyrD* strain CF1, was also eight times higher than in the parent CF1 strain when both were grown in the presence of repressing levels of uracil. When both Δ*pyrD* strains were starved for pyrimidines by growth in the presence of uridine, the level of ATCase in the Δ*pyrD* Δ*pyrR* strain CF24 was similar to, although about 15% higher than, the ATCase level in the Δ*pyrD pyrR*⁺ strain CF1 (Table 2). These findings document a requirement of the *pyrR* gene for repression of the *pyr* operon in pyrimidine-starved cells. It is noteworthy that the level of ATCase formed in the Δ*pyrD* strains CF1 and CF24 during pyrimidine-limited growth on uridine was about twice as high as that observed in cells containing the Δ*pyrR* mutations alone. This indicates that a small portion of the total derepression seen during slow growth caused by pyrimidine limitation is *pyrR* independent. Additional evidence for a component of *pyrR*-independent derepression in pyrimidine-starved cells is seen in experiments presented in Table 3, below.

Complementation of the Δ*pyrR* mutation in strains CF22 and CF24 by transformation with a *pyrR*-bearing plasmid, pFS28, restored ATCase regulation to the same pattern as observed in the *pyrR*⁺ parent strains mc²155 and CF1, respectively (Table 2). When the same strains were transformed with the vector plasmid pJEM15, they displayed the same phenotype as the Δ*pyrR* host strains. Complementation of the Δ*pyrR* chromosomal mutation by plasmid-borne *pyrR* demonstrated that the defects in regulation of *pyrB* in the Δ*pyrR* strains did

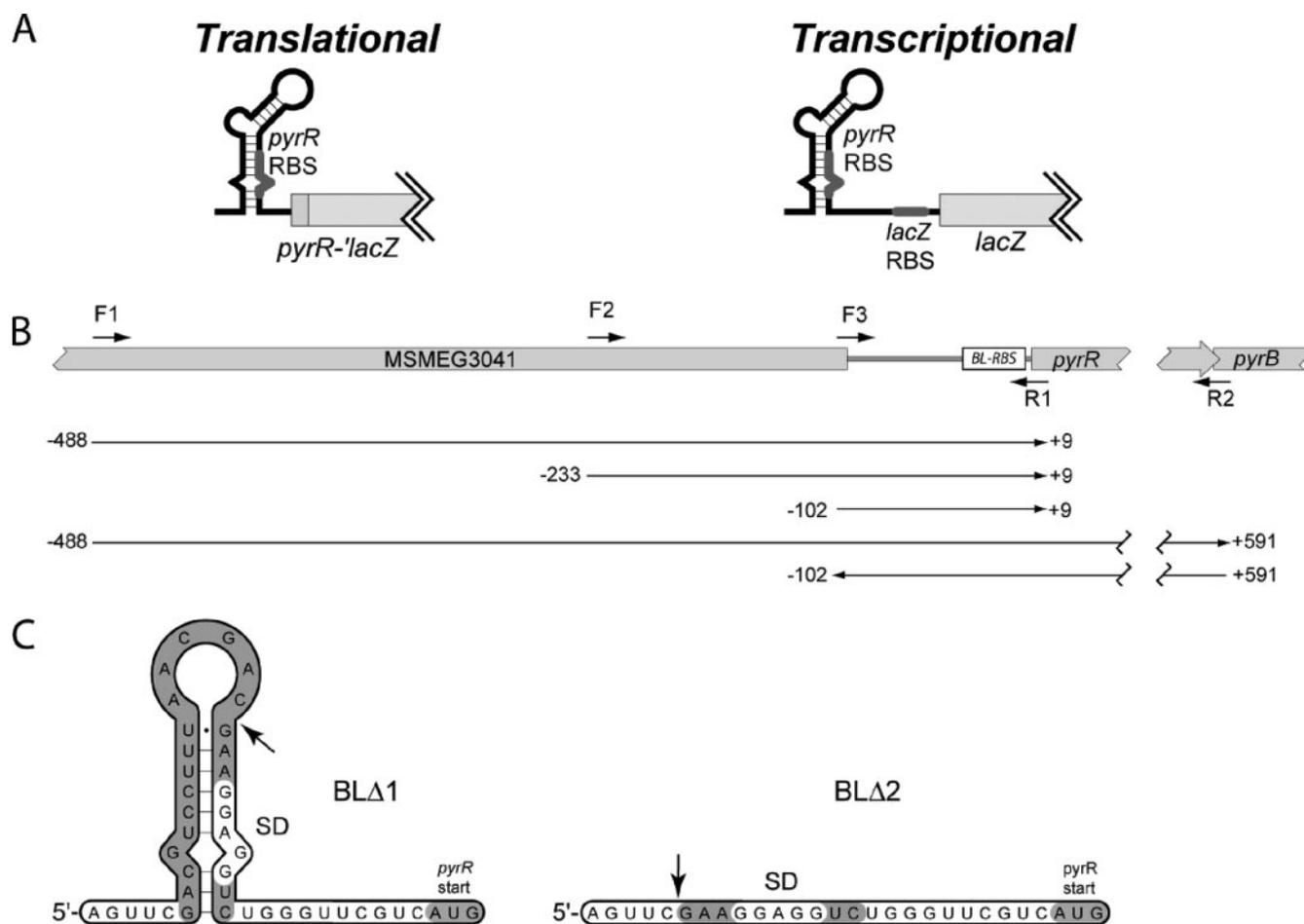FIG. 2. Construction of *pyr'-lacZ* fusion plasmids for characterization of regulation. A. Schematic diagrams showing the set of pJEM13-derived translational fusions in which the *pyr* leader, including the PyrR-binding loop region, *pyrR* ribosome-binding site (RBS), and first three codons of *pyrR* were fused in frame via a five-codon linker (Gly-Thr-Lys-Leu-Ala) to *lacZ* at codon 13 (left), and the set of pJEM15-derived transcriptional fusions in which the same *pyr* segments were fused to 56 bp of the *lacZ* leader so that the *lacZ* ribosome-binding site lies at the normal distance from the *lacZ* open reading frame (right). B. Diagram showing the locations of PCR primers (F1, F2, F3, R1, and R2) and segments of *M. smegmatis* DNA that were inserted upstream of *lacZ* to generate the plasmids described in the text and in Tables 2 and 3. Numbering of the sequence is as in Fig. 1B. C. Proposed secondary structures of the *pyr* leader RNA regions in the *pyr'-lacZ* fusion plasmids from which segments of the PyrR-binding loop were deleted (Table 3). Arrows denote the site of deletion. SD denotes the Shine-Dalgarno sequence of the presumed *pyr* ribosome-binding site.

not result from an unexpected *cis*-acting effect of constructing the deletions.

The pJEM15 plasmid used to construct the pFS28 *pyrR* complementation plasmid contained a promoterless *lacZ* gene and expressed β-galactosidase at only very low levels (Table 2). However, in the pFS28 plasmid the *lacZ* gene lies downstream from the *pyrR* insert and is under the control of the *pyr* promoter (Fig. 2). When pFS28 was expressed in strain CF22, β-galactosidase expression was elevated and was only slightly repressed by uracil (Table 2). When pFS28 was expressed under pyrimidine-limiting growth conditions in the CF24 host, β-galactosidase activity was expressed at very high levels and was repressed 13-fold by growth with uracil supplementation (Table 2). PyrR-dependent regulation of the downstream *lacZ* gene by uracil in pFS28 provides evidence for translational coupling between the upstream *pyrR* gene, whose ribosome-binding site is the putative site of PyrR action, and downstream genes (see Discussion, below).

Repression of the *pyr* operon in *M. smegmatis* is exerted at the level of mRNA translation. To analyze the mechanism of PyrR involvement in repression of *M. smegmatis pyr* gene expression by uracil, plasmids were constructed that contained the *pyr* promoter-leader region fused to a *lacZ* reporter gene in two ways. In the translational fusions the *M. smegmatis pyr* promoter and leader, which includes the putative PyrR RNA binding loop sequences and the ribosome-binding site for *pyrR* followed by the first three codons of *pyrR*, were fused in frame to codon eight of *lacZ* in pJEM13 (Fig. 2A, left). In the transcriptional fusions, the *pyr* promoter, leader, and first three codons of the *pyrR* coding sequence were fused via a 30-nucleotide linker to the native *lacZ* ribosome-binding site, followed by the complete *lacZ* gene in pJEM15 (Fig. 2A, right). Since the precise location of the *pyr* promoter was not known, in both types of fusions segments of *M. smegmatis* DNA containing 111, 242, and 497 bp directly 5′ to codon 4 of the *pyrR* open reading frame were fused to *lacZ* (Fig. 2B). This yielded

TABLE 3. Regulation of *pyr'-lacZ* transcriptional and translational fusion plasmids by pyrimidines

Strain	Relevant genotype	Plasmid	Promoter region[a]	β-Galactosidase		
				Sp act (nmol/min/mg)		Ratio
				Uracil[b]	Uridine[b]	
Translational fusions						
CF1	Δ*pyrD*	pFS4	−488 to +9	400 ± 20	7,900 ± 330	20
CF1	Δ*pyrD*	pFS5	−233 to +9	68 ± 4.1	3,200 ± 160	47
CF1	Δ*pyrD*	pFS6	−102 to +9	6.7 ± 1.2	280 ± 33	42
CF1	Δ*pyrD*	pJEM13	NA[c]	1.1 ± 0.44	0.76 ± 0.27	0.7
CF24	Δ*pyrD* Δ*pyrR*	pFS5	−233 to +9	780 ± 99	3,500 ± 440	4.5
CF1	Δ*pyrD*	pFS20	−233 to +9, with BLΔ1[d]	380 ± 21	2,000 ± 180	5.3
CF1	Δ*pyrD*	pFS21	−233 to +9, with BLΔ2[e]	1,300 ± 55	6,300 ± 430	4.8
CF24	Δ*pyrD* Δ*pyrR*	pFS20	−233 to +9, with BLΔ1	360 ± 25	1,300 ± 41	3.6
CF24	Δ*pyrD* Δ*pyrR*	pFS21	−233 to +9, with BLΔ2	1,300 ± 140	4,900 ± 550	3.8
Transcriptional fusions						
CF1	Δ*pyrD*	pFS8	−488 to +9	6,300 ± 300	15,000 ± 1,100	2.4
CF1	Δ*pyrD*	pFS9	−233 to +9	4,400 ± 180	8,800 ± 640	2.0
CF1	Δ*pyrD*	pFS10	−102 to +9	550 ± 59	1,000 ± 190	1.8
CF1	Δ*pyrD*	pJEM15	NA	2.3 ± 0.20	8.6 ± 1.6	3.7
CF24	Δ*pyrD* Δ*pyrR*	pFS9	−233 to +9	1,000 ± 77	6,500 ± 650	6.5
CF1	Δ*pyrD*	pFS22	−233 to +9, with BLΔ1	1,100 ± 15	6,900 ± 500	6.3
CF1	Δ*pyrD*	pFS23	−233 to +9, with BLΔ2	1,800 ± 75	11,000 ± 1,300	6.1
CF24	Δ*pyrD* Δ*pyrR*	pFS22	−233 to +9, with BLΔ1	870 ± 30	4,900 ± 330	5.6
CF24	Δ*pyrD* Δ*pyrR*	pFS23	−233 to +9, with BLΔ2	1,600 ± 63	8,700 ± 890	5.4

[a] Coordinates are relative to the start codon of *pyrR* as +1.
[b] Concentration in medium: uracil, 100 μg/ml; uridine 200 μg/ml.
[c] NA, not applicable.
[d] BL region with nucleotides −21 to −37 deleted.
[e] BL region with nucleotides −21 to −53 deleted.

three translational and three transcriptional *pyr-lacZ* fusion plasmids that differed only in the length of upstream DNA fused to *lacZ*. *M. smegmatis* strain CF1 (Δ*pyrD*) was transformed with all six plasmids, the transformants were grown with uracil (repressing conditions) and with uridine (pyrimidine-limiting conditions), and β-galactosidase levels were assayed to determine *pyr* promoter-directed expression (Table 3). For the translational fusions (Table 3), the derepressed β-galactosidase expression was much higher with the fusion containing a 241-bp insert than in the fusion containing the 111-bp insert, but only increased by another 2.5-fold in the fusion containing the 497-bp insert. This observation indicates that most or all of the DNA sequences needed for a fully functional *M. smegmatis pyr* promoter lie on the 241-bp segment upstream of *pyrR*. Since about 55 bp of the 3′ portion of this segment specifies the binding loop RNA, the *pyrR* ribosome-binding site, and the first three codons of *pyrR*, we suggest that the complete *pyr* promoter lies on a 180-bp segment in the 5′ portion of the 242-bp insert. A functional, but much weaker, promoter sequence lies in the 49-bp segment at the 5′ end of the 111-bp insert (see Discussion, below).

Significantly, all three inserts specified uracil-repressible activity in the translational fusion plasmids (Table 3). However, the corresponding inserts in the transcriptional fusion plasmids were repressed only about twofold by uracil (Table 3). It is shown below that this residual repression by uracil is independent of the *pyrR* gene. Thus, we conclude that the transcriptional fusion plasmids, which include the *lacZ* ribosome-binding site that is not present in the translational fusion plasmids, escape PyrR-dependent repression by uracil. Since both types of fusion plasmids contained the identical *pyr* promoter-leader

region, we conclude that uracil and PyrR exert their repressive actions by inhibition of translation at the *pyrR* ribosome-binding site, rather than acting to inhibit initiation of transcription. The most obvious mechanism for inhibition of translation is for PyrR to bind to the conserved RNA-binding loop sequences that overlap the *pyrR* ribosome-binding site. The transcriptional fusions escape repression because PyrR cannot bind to the *lacZ* ribosome-binding site.

Strain CF24 (Δ*pyrD*Δ*pyrR*) was transformed with the translational and transcriptional plasmids containing the 242-bp insert (pFS5 and pFS9, respectively), and β-galactosidase levels were determined in cells grown in the presence of uracil and uridine to assess the role of the *pyrR* gene in regulation of expression of the *pyr'-lacZ* plasmids. The ability of uracil to repress expression of the *pyr'-lacZ* fusion translation was largely abolished in the Δ*pyrR* background, as shown by the 11-fold increase in β-galactosidase level formed in CF24 cells compared to that produced from the same plasmid in *pyrR*^{+} cells (Table 3, CF1 with pFS5 grown with uracil versus CF24 with pFS5). On the other hand, β-galactosidase expression, which was elevated and poorly repressed by uracil in the transcriptional *pyr'-lacZ* fusion, was also poorly regulated in the Δ*pyrR* host (Table 3, CF1 with pFS9 versus CF24 with pFS9). These observations confirm that regulation of expression of the *pyr'-lacZ* fusion by uracil was largely dependent on the *pyrR* gene. However, there was a *pyrR*-independent component to the increased expression of β-galactosidase seen with these plasmids during pyrimidine-limited growth, as indicated by the 4.5- to 6.5-fold higher levels seen in CF24 cells grown with uridine versus CF24 cells grown with uracil.

TABLE 4. Expression of alternative *lacZ* transcriptional fusion plasmids under pyrimidine-limiting conditions

Strain	Relevant genotype	Plasmid	Promoter	β-Galactosidase		
				Sp act (nmol/min/mg)		Ratio
				Uracil[a]	Uridine[a]	
CF1	Δ*pyrD*	pFS30	*MSMEG3041*	380 ± 14	1,100 ± 100	2.9
CF1	Δ*pyrD*	pFS31	*Ag85A* (*fbpA*)	77 ± 6.6	120 ± 21	1.6
CF1	Δ*pyrD*	pFS32	*hsp60* (*groEL2*)	8,300 ± 420	25,000 ± 2,200	3.0
CF24	Δ*pyrD* Δ*pyrR*	pFS30	*MSMEG3041*	450 ± 30	1,000 ± 170	2.2
CF24	Δ*pyrD* Δ*pyrR*	pFS31	*Ag85A* (*fbpA*)	57 ± 3.5	77 ± 8.3	1.4
CF24	Δ*pyrD* Δ*pyrR*	pFS32	*hsp60* (*groEL2*)	7,500 ± 180	21,000 ± 1,700	2.8

[a] Concentrations in medium: uracil, 100 μg/ml; uridine, 200 μg/ml.

Repression of the *pyr* operon in *M. smegmatis* requires an intact PyrR-binding site adjacent to the *pyrR* ribosome-binding site in the *pyr* transcript. If PyrR acts to repress *pyr* operon expression by binding to the conserved RNA-binding loop sequences in the *pyr* leader, as we have proposed, *pyr'-lacZ* translational fusion plasmids from which DNA specifying portions of the binding loop RNA has been deleted should no longer be repressed by uracil. Effects of uracil on expression of transcriptional fusions, from which the same binding loop sequences are deleted but which still contain the *lacZ* ribosome-binding site, should be small and similar to those seen with the corresponding plasmids from which the binding loop sequences are not deleted. These predictions were tested with translational fusion plasmids pFS20 and pFS21 (Table 3) and transcriptional fusion plasmids pFS22 and pFS23 (Table 3). In pFS20 and pFS22, a 17-bp segment specifying nucleotide −37 to −21 of the binding loop RNA (BLΔ1) was deleted; in pFS21 and pFS23 the entire binding loop upstream of the putative *pyrR* ribosome-binding site (−53 to −21; BLΔ2) was deleted (Fig. 1B and 2C). In all of the plasmids the putative *pyrR* Shine-Dalgarno sequence (−13 to −17) was retained. All four binding loop deletion plasmids were introduced separately into strain CF1 (Δ*pyrD*), and β-galactosidase levels were determined in cells grown with uracil and uridine as pyrimidine sources. Deletion of the binding loop sequences sharply reduced the ability of uracil to repress expression in the translational fusion plasmids pFS20 and pFS21 (about fivefold repression) (Table 3) compared to the corresponding translational fusion plasmid pFS5 (47-fold) (Table 3) from which the binding loop was not deleted. Effects of uracil and uridine on expression of the transcriptional fusion plasmids containing binding loop deletions, pFS22 and pFS23 (Table 3), were similar to those seen with the parent plasmid pFS9 (Table 3), although repression ratios were actually somewhat higher (sixfold versus twofold) with the transcriptional fusion plasmids with binding loop deletions. These results confirm a requirement for the PyrR-binding loop sequence for strong repression by uracil. Curiously, the expression of all of the plasmids was elevated by five- to sixfold in uridine-grown cells, which is greater than the two- to threefold elevation of ATCase expression observed in pyrimidine-starved Δ*pyrR* cells (Table 2). This might suggest that some residual PyrR-dependent regulation occurs even when the binding loop is deleted. However, the experiments in Table 3 using strain CF24 (Δ*pyrD* Δ*pyrR*) transformed with pFS20, pFS21, pFS23, and pFS23 demonstrated that the four- to sixfold derepression observed in cells grown

under pyrimidine-limiting conditions was independent of the *pyrR* gene.

Effects of pyrimidine-limited growth on expression controlled by other *M. smegmatis* promoters. The highest expression of the *M. smegmatis pyr* genes was obtained in our studies when Δ*pyrD* host cells were starved for pyrimidines by slow growth on uridine. From the data in Table 2 it is seen that most of the derepression of *pyrB* (ATCase) under these conditions requires the *pyrR* gene, but two- to threefold derepression occurs in Δ*pyrR* strains. In studies with *pyr'-lacZ* fusion plasmids, the *pyrR*-independent component of derepression in uridine-grown cells was usually higher, generally four- to sixfold (Table 3). Does the *pyrR*-independent component of derepression represent a second mode of regulation of *pyr* genes by uracil, or does it result from a general, nonspecific effect of slow growth during pyrimidine starvation? We attempted to address this question by examining the effects of pyrimidine starvation on expression of three plasmids in which the *hsp60* (*groEL2*) (10, 26), *Ag85* (*fbpA*) (2, 26), and putative MS-MEG3041 (see Materials and Methods) promoters were transcriptionally fused to *lacZ* in pJEM15. We reasoned that a second mechanism that was specific for regulation of *pyr* gene expression, if such a mechanism existed, would act on the *pyr* promoter but not on promoters that have no function in nucleotide metabolism. Strain CF1 and CF24 cells were transformed with the new promoter-*lacZ* fusion plasmids, the cells were grown with uracil and uridine as in the experiments of Tables 2 and 3, and β-galactosidase expression was assayed. Expression of two of the promoter fusion plasmids was elevated by about threefold in the cells grown under pyrimidine limitation (Table 4), whether or not the host strain contained a functional *pyrR* gene. Expression of the *Ag85-lacZ* fusion plasmid was also elevated during pyrimidine-limited growth, but to a lesser extent. We conclude that most of the *pyrR*-independent derepression previously observed with the *pyr'-lacZ* fusion plasmids was a nonspecific effect of slow growth or depleted intracellular pyrimidine nucleotide levels (see Discussion).

DISCUSSION

Location and properties of the *M. smegmatis pyr* promoter. Although the site of transcription initiation has not been mapped precisely for the *M. smegmatis pyr* operon by primer extension, our experiments with *pyr'-lacZ* fusion plasmids demonstrated that a functional pyrimidine-regulated *pyr* pro-
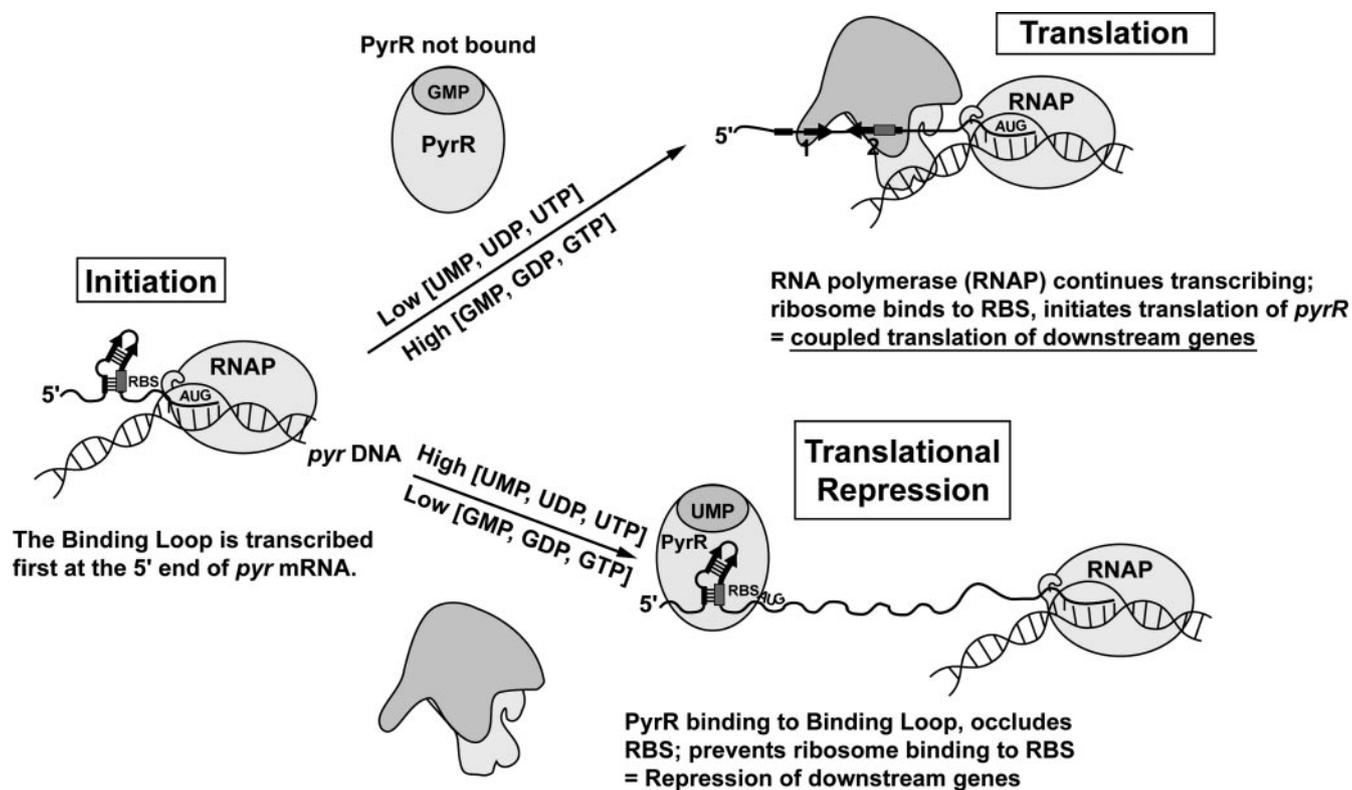
FIG. 3. Proposed mechanism of PyrR-mediated regulation of the *M. smegmatis pyr* operon by translational repression.

moter lies in a 72-bp segment of DNA lying from 55 to 102 bp 5′ to the start of *pyrR* translation (Fig. 1B). Within this region a consensus sequence (TANNNT) for the −10 region mycobacterial promoters (1) is found at −66 to −71 (TAAGCT), with numbering from the start of translation. Separated by 18 bp upstream at −90 to −95, the sequence TTCCCC is found, which matches the mycobacterial −35 consensus sequence (TTGCGA) (1) in three of six positions. These sequences would predict a likely start for *pyr* transcription 7 or 8 bp downstream from the −10 sequence at A-58 or G-57, just 4 or 5 bp before the sequence that specifies the beginning of the PyrR-binding loop RNA. Possibly as a result of the relatively weak −35 sequence, the core promoter sequence located in the 111-bp *pyr′-lacZ* fusion plasmid pFS6 supported 10- and 20-fold lower expression, respectively, than the 242-bp (pFS5) and 497-bp (pFS4) *pyr′-lacZ* fusion plasmids (Table 3). This suggests that upstream elements, while not part of the core promoter, serve to activate *pyr* transcription in *M. smegmatis*. The activation of the *M. smegmatis rrnB* operon by upstream elements provides precedence for such a phenomenon (3), but the specific sequences involved in *rrnB* activation are not found upstream of the *pyr* operon.

A model for regulation of the *M. smegmatis pyr* operon by PyrR-dependent translational repression. Our experiments demonstrated that most of the repressive effects of exogenous uracil on *pyr* expression in *M. smegmatis* required both the *pyrR* gene and the presence of the PyrR-binding loop RNA sequence that lies in the untranslated leader upstream of the *pyrR* gene. Furthermore, this regulatory effect was largely abolished if a second ribosome-binding site that does not overlap

the PyrR binding sequence was provided for the *lacZ* reporter gene. We propose that a translational repression model for PyrR action in *M. smegmatis* accounts for these observations (Fig. 3). According to this model, PyrR binding to its specific binding site in the *pyr* leader is stimulated by high levels of uridine nucleotides and antagonized by high levels of guanosine nucleotides, as has been demonstrated for the *Bacillus* PyrR (8). We have also demonstrated these effects of nucleotides on the binding of purified PyrR from *M. tuberculosis* to *M. tuberculosis* binding loop RNA (C. J. Fields and R. L. Switzer, unpublished data). When PyrR is not bound, ribosomes are able to bind to a site just upstream of the *pyrR* open reading frame and initiate translation. However, the PyrR-binding site and the Shine-Dalgarno sequence of the *pyrR* ribosome-binding site overlap, and so when PyrR is bound at high uridine nucleotide concentrations, binding of ribosomes is inhibited and translation is repressed. Although competition between ribosomes and PyrR would occur only at a site upstream of *pyrR*, the first cistron of the *pyr* operon, translation of all of the downstream *pyr* genes might also be inhibited because of translational coupling. Evidence that such translational coupling occurs is seen from the efficient regulation of the expression of *pyrB*, the second cistron of the operon by exogenous uracil (Table 2), and by similar regulation of *lacZ* when this gene lies artificially downstream from *pyrR* in the *pyrR* complementation plasmid pFS28 (Table 2). Transcriptional polarity of the polycistronic *pyr* mRNA could also affect expression of the downstream genes. Further testing of the proposed model by biochemical experiments is in progress in our laboratory.

The nature of PyrR-independent derepression during growth under pyrimidine-limiting conditions. Addition of uracil to defined pyrimidine-free medium gave only a twofold decrease in *pyrB* expression in *M. smegmatis*, and so it was necessary to grow a pyrimidine auxotroph on uridine, which resulted in slow growth and consequent derepression of *pyrB*, to demonstrate the full extent of repression by uracil. Such a device is commonly used to study regulation of bacterial biosynthetic genes. Full derepression of the *B. subtilis pyr* operon (19) and *pyrG* (23) required growth of auxotrophs on orotate, which supports slow pyrimidine-limited growth in that organism. Most of the derepression of *pyrB* or *pyr′-lacZ* fusion plasmids seen in *M. smegmatis* grown under pyrimidine-limiting conditions was dependent on the *pyrR* gene, but a residual portion, ranging from two- to sixfold, was observed in Δ*pyrR* strains (Tables 2 and 3). The experiments reported in Table 4 document that threefold derepression of two other *M. smegmatis* promoters, whose functions are unrelated to pyrimidine metabolism, was observed under the same conditions of pyrimidine-limited growth. Thus, this effect reflects, largely if not entirely, a generalized and nonspecific effect of such growth conditions on gene expression and is not the reflection of a second PyrR-independent regulatory mechanism that specifically governs *pyr* gene expression. The biochemical basis of this effect is not clear. It could represent a generalized stress response induced by slow growth, or it could be mediated by the low intracellular concentrations of pyrimidine nucleotides under these conditions. It is noteworthy that a similar two- to threefold effect of slow growth of *B. subtilis* pyrimidine auxotrophs on orotate was observed for the *pyr* operon in a Δ*pyrR* strain (19) and for the *pyrG* gene in a strain in which the 5′ leader attenuator was deleted (23).

Translational repression of *pyr* genes by PyrR in other species. The *pyr* genes of *M. tuberculosis* (9) and other mycobacteria (7, 32) are organized into operons in which the first cistron is *pyrR* and the 5′ leader sequences include a PyrR-binding loop that overlaps a putative ribosome-binding site in the same way as seen in *M. smegmatis*. It seems very likely, therefore, that the *pyr* operons in these species are regulated by a translational repression mechanism like that described here.

A review of published genome sequences indicated that *pyrR* genes and PyrR-binding sequences that overlap the ribosome-binding sites for *pyr* genes are quite widespread in other bacterial species. Often when this arrangement is found, attenuator terminator and antiterminator sequences are not present downstream from the PyrR-binding sequence, which argues against a transcription attenuation regulatory mechanism for such genes. Our findings in this work provide support for the idea that such arrangements indicate likely regulation of these genes by translational repression, although they do not, of course, demonstrate that this is the case. C. J. Fields (unpublished) has identified a number of species in which open reading frames for putative *pyrP* (*uraA*) genes encoding uracil transporters and/or another putative transport protein of the major facilitator protein superfamily fit this pattern. In some species (e.g., *Clostridium* spp.) this arrangement coexists with *pyr* genes that are regulated by PyrR-mediated transcriptional attenuation. In other cases (e.g., *Haemophilus influenzae*, *Pasteurella multocida*), translational repression of the genes for transport proteins and/or *carA* appears to be the only mode of

PyrR regulation. A regulatory mechanism involving both PyrR-dependent translational repression and transcription attenuation has been proposed for *Thermus* strain ZO5 and related *Thermus* species (37). In *Thermus* strain ZO5 an open reading frame for short leader polypeptide precedes the *pyrR* gene and other downstream genes of a *pyr* operon. The ribosome-binding site in the mRNA for the leader polypeptide overlaps a consensus PyrR-binding sequence so that translational repression by PyrR is likely. The RNA encoding the leader polypeptide is also capable of forming a transcription terminator. Van de Casteele et al. (37) suggested that attenuation at this terminator is regulated by the rate of translation of the leader polypeptide, which is in turn responsive to pyrimidines via PyrR-mediated translational repression. Furthermore, 6 of 28 codons in the leader polypeptide encode arginine, which might account for stimulation of *pyr* gene expression in *Thermus* strain ZO5 by this amino acid. This interesting model has not yet been tested by genetic or biochemical means, however. Altogether, these observations indicate that translational repression by PyrR may be as widespread among bacteria as PyrR-dependent transcription attenuation and may have preceded it in evolutionary development.

Translational repression is a widespread regulatory mechanism in prokaryotes. Numerous examples of the regulation of genes by translational repression by various mechanisms have been reported (29). Of these examples, translational repression of the *B. subtilis trpG* (11), *trpP* (39), and *ycbK* (38) genes by the *trp* RNA-binding attenuation protein TRAP (5) presents a close analogy to the mechanism we have proposed for regulation of *pyr* genes by *M. smegmatis* PyrR. Like PyrR, TRAP also regulates gene expression by a transcription attenuation mechanism (5). However, in the cases cited, strong evidence has been presented that TRAP acts to inhibit translation initiation by binding to mRNA at the ribosome-binding site. Remarkably, TRAP can also inhibit translation of the *trpE* gene by binding to a site that does not overlap the ribosome-binding site but instead favors an alternative fold of *trpE* RNA that occludes the ribosome-binding site in a hairpin structure (5). We suspect that numerous additional examples and mechanistic variations of translational repression mechanisms remain to be discovered.

REFERENCES

1. **Agarwal, N., and A. K. Tyagi.** 2006. Mycobacterial transcription signals: requirements for recognition by RNA polymerase and optimal transcriptional activity. Nucleic Acids Res. **34:**4245–4257.
2. **Armitige, L. Y., C. Jagannath, A. R. Wanger, and S. J. Norris.** 2000. Disruption of the genes encoding antigen 85A and antigen 85B of *Mycobacterium tuberculosis* H37Rv: effect on growth in culture and in macrophages. Infect. Immun. **68:**767–778.
3. **Arnvig, K. B., B. Gopal, K. G. Papavinasasundaram, R. A. Cox, and M. J. Colston.** 2005. The mechanism of upstream activation in the *rrnB* operon of *Mycobacterium smegmatis* is different from the *Escherichia coli* paradigm. Microbiology **151:**467–473.

4. **Arsene-Ploetz, F., V. Kugler, J. Martinussen, and F. Bringel.** 2006. Expression of the *pyr* operon of *Lactobacillus plantarum* is regulated by inorganic carbon availability through a second regulator, PyrR$_2$, homologous to the pyrimidine regulator PyrR$_1$. J. Bacteriol. **188:**8607–8616.

5. **Babitzke, P., and P. Gollnick.** 2001. Posttranscription initiation control of tryptophan metabolism in *Bacillus subtilis* by the *trp* RNA-binding attenuation protein (TRAP), anti-TRAP, and RNA structure. J. Bacteriol. **183:**5795–5802.

6. **Bonner, E. R., J. N. D'Elia, B. K. Billips, and R. L. Switzer.** 2001. Molecular recognition of *pyr* mRNA by the *Bacillus subtilis* attenuation regulatory protein PyrR. Nucleic Acids Res. **29:**4851–4865.

7. **Brosch, R., S. V. Gordon, T. Garnier, et al.** 2007. Genome plasticity of BCG and impact on vaccine efficacy. Proc. Nat. Acad. Sci. USA **104:**5596–5601.

8. **Chander, P., K. M. Halbig, J. K. Miller, C. J. Fields, H. K. S. Bonner, G. K. Grabner, R. L. Switzer, and J. L. Smith.** 2005. Structure of the nucleotide complex of PyrR, the *pyr* attenuation protein from *Bacillus caldolyticus*, suggests dual regulation by pyrimidine and purine nucleotides. J. Bacteriol. **187:**1773–1782.

9. **Cole, S. T., R. Brosch, J. Parkhill, et al.** 1998. Deciphering the biology of *Mycobacterium tuberculosis* from the complete genome sequence. Nature **393:**537–544.

10. **Dellagostin, O. A., G. Esposito, L. J. Eales, J. W. Dale, and J. McFadden.** 1995. Activity of mycobacterial promoters during intracellular and extracellular growth. Microbiology **141:**1785–1792.

11. **Du, H., R. Tarpey, and P. Babitzke.** 1997. The *trp* RNA-binding attenuation protein regulates TrpG synthesis by binding to the *trpG* ribosome binding site of *Bacillus subtilis*. J. Bacteriol. **179:**2582–2586.

12. **Elagöz, A., A. Abdi, J.-C. Hubert, and B. Kammerer.** 1996. Structure and organisation of the pyrimidine biosynthesis pathway genes in *Lactobacillus plantarum*: a PCR strategy for sequencing without cloning. Gene **182:**37–43.

13. **Ghim, S.-Y., C. C. Kim, E. R. Bonner, J. N. D'Elia, G. K. Grabner, and R. L. Switzer.** 1999. The *Enterococcus faecalis pyr* operon is regulated by autogenous transcriptional attenuation at a single site in the 5′ leader. J. Bacteriol. **181:**1324–1329.

14. **Ghim, S.-Y., and J. Neuhard.** 1994. The pyrimidine biosynthesis operon of the thermophile *Bacillus caldolyticus* includes genes for uracil phosphoribosyltransferase and uracil permease. J. Bacteriol. **176:**3698–3707.

15. **Hinds, J., E. Mahenthiralingam, K. E. Kempsell, K. Duncan, R. W. Stokes, T. Parish, and N. G. Stoker.** 1999. Enhanced gene replacement in mycobacteria. Microbiology **145:**519–527.

16. **Hoang, T. T., R. R. Karkhoff-Schweizer, A. J. Kutchma, and H. P. Schweizer.** 1998. A broad-host-range Flp-FRT recombination system for site-specific excision of chromosomally-located DNA sequences: application for isolation of unmarked *Pseudomonas aeruginosa* mutants. Gene **212:**77–86.

17. **Lu, Y., and R. L. Switzer.** 1996. Transcriptional attenuation of the *Bacillus subtilis pyr* operon by the PyrR regulatory protein and uridine nucleotides in vitro. J. Bacteriol. **178:**7206–7211.

18. **Lu, Y., R. J. Turner, and R. L. Switzer.** 1996. Function of the RNA secondary structures in the regulation of the *Bacillus subtilis pyr* operon expression. Proc. Natl. Acad. Sci. USA **93:**14462–14467.

19. **Lu, Y., R. J. Turner, and R. L. Switzer.** 1995. Roles of the three transcriptional attenuators of the *Bacillus subtilis* pyrimidine biosynthetic operon in the regulation of its expression. J. Bacteriol. **177:**1315–1325.

20. **Martinussen, J., and K. Hammer.** 1998. The *carB* gene encoding the large subunit of carbamoylphosphate synthetase from *Lactococcus lactis* is transcribed monocistronically. J. Bacteriol. **180:**4380–4386.

21. **Martinussen, J., J. Schallert, B. Andersen, and K. Hammer.** 2001. The pyrimidine operon *pyrRPB-carA* from *Lactococcus lactis*. J. Bacteriol. **183:**2785–2794.

22. **Masood, R., and T. A. Venkitasubramanian.** 1988. Purification and properties of aspartate transcarbamylase from *Mycobacterium smegmatis*. Biochim. Biophys. Acta **953:**106–113.

23. **Meng, Q., and R. L. Switzer.** 2001. Regulation of transcription of the *Bacillus subtilis pyrG* gene encoding cytidine triphosphate synthetase. J. Bacteriol. **183:**5513–5522.

24. **Miller, J. H.** 1972. Experiments in molecular genetics. Cold Spring Harbor Laboratory, Cold Spring Harbor, NY.

25. **Nicoloff, H., A. Elagoz, F. Arsene-Ploetze, B. Kammerer, J. Martinussen, and F. Bringel.** 2005. Repression of the *pyr* operon in *Lactobacillus plantarum* prevents its ability to grow at low carbon dioxide levels. J. Bacteriol. **187:**2093–2104.

26. **Parish, T., and N. G. Stoker.** 2000. Use of a flexible cassette method to generate a double unmarked *Mycobacterium tuberculosis tlyA plcABC* mutant by gene replacement. Microbiology **146:**1969–1975.

27. **Perbal, B., and G. Herve.** 1972. Biosynthesis of *Escherichia coli* aspartate transcarbamylase I. Parameters of gene expression and sequential biosynthesis of the subunits. J. Mol. Biol. **70:**511–529.

28. **Sambrook, J., E. F. Fritsch, and T. Maniatis.** 1989. Molecular cloning: a laboratory manual. Cold Spring Harbor Laboratory Press, Cold Spring Harbor, NY.

29. **Schlax, P. J., and D. J. Worhunsky.** 2003. Translational repression mechanisms in prokaryotes. Mol. Microbiol. **48:**1157–1169.

30. **Schweizer, H. D.** 1993. Small broad-host-range gentamycin resistance gene cassettes for site-specific insertion and deletion mutagenesis. BioTechniques **15:**831–834.

31. **Snapper, S. B., R. E. Melton, S. Mustafa, T. Kieser, and W. R. Jacobs.** 1990. Isolation and characterization of efficient plasmid transformation mutants of *Mycobacterium smegmatis*. Mol. Microbiol. **4:**1911–1919.

32. **Stinear, T. P., T. Seemann, S. Pidot, et al.** 2007. Reductive evolution and niche adaptation inferred from the genome of *Mycobacterium ulcerans*, the causative agent of Buruli ulcer. Genome Res. **17:**192–200.

33. **Switzer, R. L., R. J. Turner, and Y. Lu.** 1999. Regulation of the *Bacillus subtilis* pyrimidine biosynthetic operon by transcriptional attenuation: control of gene expression by an mRNA-binding protein. Prog. Nucleic Acids Res. Mol. Biol. **62:**329–367.

34. **Timm, J., E. M. Lim, and B. Gicquel.** 1994. *Escherichia coli*-mycobacteria shuttle vectors for operon and gene fusions to *lacZ*: the pJEM series. J. Bacteriol. **176:**6749–6753.

35. **Turner, R. J., E. R. Bonner, G. K. Grabner, and R. L. Switzer.** 1998. Purification and characterization of *Bacillus subtilis* PyrR, a bifunctional *pyr* mRNA-binding attenuation protein/uracil phosphoribosyltransferase. J. Biol. Chem. **273:**5932–5938.

36. **Turner, R. J., Y. Lu, and R. L. Switzer.** 1994. Regulation of the *Bacillus subtilis* pyrimidine biosynthetic (*pyr*) gene cluster by an autogenous transcriptional attenuation mechanism. J. Bacteriol. **176:**3708–3722.

37. **Van de Casteele, M., P. Chen, M. Roovers, C. Legrain, and N. Glansdorff.** 1997. Structure and expression of a pyrimidine gene cluster from the extreme thermophile *Thermus* strain ZO5. J. Bacteriol. **179:**3470–3481.

38. **Yakhnin, H., A. V. Yakhnin, and P. Babitzke.** 2006. The *trp* RNA-binding attenuation protein (TRAP) of *Bacillus subtilis* regulates translation initiation of *ycbK*, a gene encoding a putative efflux protein, by blocking ribosome binding. Mol. Microbiol. **61:**1252–1266.

39. **Yakhnin, H., H. Zhang, A. V. Yakhnin, and P. Babitzke.** 2004. The *trp* RNA-binding attenuation protein of *Bacillus subtilis* regulates translation of the tryptophan transport gene *trpP* (*yhaG*) by blocking ribosome binding. J. Bacteriol. **186:**278–286.